

See discussions, stats, and author profiles for this publication at: <https://www.researchgate.net/publication/228481585>

Near-Infrared Electrochromic and Electroluminescent Polymers Containing Pendant Ruthenium Complex Groups

ARTICLE *in* MACROMOLECULES · OCTOBER 2006

Impact Factor: 5.8 · DOI: 10.1021/ma061751+

CITATIONS

35

READS

10

5 AUTHORS, INCLUDING:



[Zhi Yuan Wang](#)

Carleton University

196 PUBLICATIONS 3,242 CITATIONS

SEE PROFILE

Near-Infrared Electrochromic and Electroluminescent Polymers Containing Pendant Ruthenium Complex Groups

Sheng Wang,[‡] Xianzhen Li,[†] Shidi Xun,[†] Xinhua Wan,^{*,‡} and Zhi Yuan Wang^{*,‡}

Beijing National Laboratory for Molecular Sciences, Key Laboratory of Polymer Chemistry and Physics of the Ministry of Education, College of Chemistry and Molecular Engineering, Peking University, Beijing 100871, China, and Department of Chemistry, Carleton University, 1125 Colonel By Drive, Ottawa, Ontario, Canada K1S 5B6

Received August 2, 2006; Revised Manuscript Received August 30, 2006

ABSTRACT: A series of near-infrared (NIR) electrochromic and electroluminescent polymers containing the pendant dinuclear ruthenium complexes were synthesized and characterized. All the polymers are near-infrared (NIR) electrochromic, displaying an intense absorption centered at 1600 nm upon oxidation to the mixed-valence state. Single-layer diode devices comprising a layer of the complex polymers sandwiched between the ITO and Au electrodes emitted the NIR light centered at 790 nm at ambient temperature.

Introduction

Organic optoelectronic materials that can absorb and produce light efficiently in the near-infrared region (800–2000 nm) are potentially useful for telecommunications (1300–1600 nm), thermal imaging (>1500 nm), biological imaging (800–1100 nm), and solar cells (800–2000 nm). The use of NIR light in tissue imaging allows for deeper depth of detection than visible light and reduces the autofluorescence and absorption of biological species (e.g., hemoglobin) and water. NIR light centered at 840 nm or longer wavelengths can effectively penetrate tissues and enable optical detection in depths over 5 cm.¹ Among several types of NIR organic materials, a family of dinuclear ruthenium complexes (DCH–Ru) with a dicarbonylhydrazine (DCH) bridging ligand are particularly interesting as a new class of NIR organic materials. The early work on DCH–Ru complexes by Kaim et al. revealed NIR electrochromism of these complexes.² Recent studies showed the structure–property relationship between the substituent groups and the NIR absorption and demonstrated a potential application for attenuation of light at the telecommunication wavelength (1310 and 1550 nm).^{3,4} DCH–Ru complexes can exist in three forms depending on the oxidation state of ruthenium metals: Ru^{II}/Ru^{II}, Ru^{II}/Ru^{III}, and Ru^{III}/Ru^{III}. Accordingly, the absorption bands are typically centered at 550 nm (Ru^{II}/Ru^{II}), 800 nm (Ru^{III}/Ru^{III}), and 1600 nm (Ru^{II}/Ru^{III}) and assigned to the metal-to-ligand charge transfer (MLCT), ligand-to-metal charge transfer (LMCT), and metal-to-metal charge transfer (MMCT) transitions. A device for NIR optical attenuation has been demonstrated by utilizing the electrochromic (EC) switch between the Ru^{II}/Ru^{II} and Ru^{II}/Ru^{III} states and a high absorption of the mixed-valence state in the NIR region.^{3d,e}

NIR emission is of both academic and commercial interest due to potential applications in optical sensors and telecommunications.^{5,6} To date, extensive studies have been carried out on the photoluminescence (PL) and electroluminescence (EL) of mononuclear ruthenium complexes, and most of the mono-

nuclear ruthenium complexes emit orange-red light with emission peaks at 600–650 nm.^{7–9} Although NIR PL properties of a few dinuclear ruthenium complexes have been studied, no NIR EL emission have been reported.^{10–12} For example, Kol et al.¹⁰ and Lehn et al.¹¹ synthesized some dinuclear ruthenium complexes and only demonstrated triplet metal–ligand-charge-transfer (³MLCT) PL emission at 1028–1100 and 840–950 nm, respectively.

Furthermore, in comparison with ruthenium complexes,^{7–13} the polymers containing ruthenium complexes have received much less attention for their PL and EL properties.¹⁴ As emitters in a device, polymers can offer many advantages over small-molecule systems including better processing capability, film quality, and better control over morphology. In 1997, Rubner et al. first reported the use of polymers containing mononuclear ruthenium complexes as emitters in solid-state devices and some interesting EL properties.^{14a} There is still no report on the polymers containing dinuclear ruthenium complexes as active NIR emitters in LED devices.

In this paper, we report the synthesis of a series of polymers containing dinuclear ruthenium complexes (DCH–Ru) as pendant groups and the NIR EC, PL, and EL properties of these complex polymers.

Experimental Section

General Methods. All manipulations involving air-sensitive reagents were performed in an atmosphere of dry argon. All reagents, unless otherwise specified, were obtained from Aldrich and Acros and were used as received. All solvents were carefully dried and purified under nitrogen. Infrared spectra of the samples in pressed KBr pellets were recorded on a Bio-Rad FTS 165 FT-IR spectrophotometer. ¹H and ¹³C NMR spectra were recorded on a Bruker DRX 400 spectrometer operating at 400 and 100 MHz, respectively, and were referenced to tetramethylsilane. Molecular weights and polydispersity index (PDI) of the polymers were measured relative to polystyrene standards with a Waters GPC 2410 instrument using tetrahydrofuran. Elemental analyses were performed on Vario EL elemental analysis instrument. Thermogravimetric analyses (TGA) of polymer powders were done on a TA Instruments SDT 2960 with a heating rate of 10 °C/min under an air flow of 75 cm³/min. Glass transition temperatures of the polymers were measured by differential scanning calorimetry (DSC)

* Corresponding authors. E-mail: wayne_wang@carleton.ca and xhwan@pku.edu.cn.

[†] Carleton University.

[‡] Peking University.

Table 1. Characterization of Ligand Polymers 3 and Complex Polymers 4

ligand polymer	monomer ratio ^a	monomer ratio ^b	$M_n \times 10^{-4}$ ^c	PDI ^c	complex polymer	Ru content ^d
3a	1:6.5	1:19	4.2	2.2	4a	4.0
3b	1:4	1:5.2	2.8	2.4	4b	4.9
3c	1:3	1:4.3	2.8	2.2	4c	9.2
3d	1:2	1:3.2	2.4	2.4	4d	10.1

^a Mole ratio of ligand group to carbazole group in feed in polymerization. ^b Mole ratio of ligand group to carbazole group in polymers determined by elemental analysis. ^c Number-average molecular weight obtained by GPC relative to polystyrene standards in THF. ^d Obtained by ICP analysis.

on a TA Instruments Q100 from 30 to 280 °C at a heating rate of 10 °C/min under a continuous nitrogen flow. The UV-vis-NIR absorption spectra were recorded on a Lambda 900 Perkin-Elmer spectrophotometer. Cyclic voltammograms (CV) were recorded on a BAS 100 electrochemical workstation with platinum electrodes against a silver pseudoreference electrode with nitrogen-saturated solution of 0.1 M tetra-*n*-butylammonium hexafluorophosphate (Bu₄NPF₆) in acetonitrile. The spectroelectrochemical measurements were performed in an optical transparent thin layer (OTTLE) cell. The single-layer LED devices having the structure of ITO/complex polymer/Au were fabricated by spin-coating of polymer solution on indium tin oxide (ITO)-covered glass substrates, followed by thermal evaporation of a layer of gold as a cathode onto the polymer layer. The thickness of the complex polymer layer is typically controlled to be 80 nm. The PL and EL spectra were collected using a Keithley 236 source meter and PTI fluorescence instrument.

4-Vinylbenzoic Acid. 4-Bromomethylbenzoic acid (8.60 g),^{16a} triphenylphosphine (11.54 g, 44.0 mmol), and 150 mL of acetone were placed into a 250 mL round-bottomed flask. The solution was heated to reflux for 6 h. After cooling to room temperature, the product was collected by filtration and was washed with cold acetone several times. The dried phosphonium salt (14.6 g, 30.6 mmol, 82% yield) was dissolved in 310 mL of 40% formaldehyde solution, followed by addition of 192 mL of 2.5 M NaOH solution dropwise. After stirring at room temperature overnight, the resulting solid was removed by filtration, and the filtrate was acidified to yield the desired product as a white solid (3.30 g, 73%). ¹H NMR (400 MHz, DMSO-*d*₆) δ (ppm): 12.88 (s, 1H, -COOH), 7.94 (d, 2H, ph-H), 7.61 (d, 2H, ph-H), 6.80 (q, 1H, ph-CH=), 6.01 (d, 1H, =CH), 5.44 (d, 1H, =CH).

Monomer 1. 4-Vinylbenzoic acid (7.50 g, 50.6 mmol) was dissolved in 200 mL of oxalyl chloride, followed by addition of several drops of DMF. After stirring 3 days at room temperature, the solvent was evaporated, and the residual liquid (acid chloride) was used in the next step without further purification. The acid chloride obtained above (25.0 mmol) and triethylamine (4 mL, 29.0 mmol) were dissolved in 30 mL of DMF, followed by addition of a solution of benzoyl hydrazine (3.57 g, 26.3 mmol) in 30 mL of DMF. After stirring overnight the resulting salt was removed by filtration. The filtrate was poured into water, and the resulting solid product was collected by filtration and purified by column chromatography (dichloromethane and ethyl acetate, 6:1 v/v): 4.60 g (70%). ¹H NMR (400 MHz, DMSO-*d*₆) δ (ppm): 10.52 (s, 2H, -NH), 7.95 (m, 4H, ph-H), 7.65 (m, 5H, ph-H), 6.82 (q, 1H, ph-CH=), 6.01 (d, 1H, =CH), 5.44 (d, 1H, =CH). MS (EI, *m/z*): 266. Anal. Calcd: C 72.16%, H 5.30%, N 10.52%. Found: C 71.46%, H 5.31%, N 10.29%. IR (KBr, cm⁻¹): 3204–3009 (NH), 1672 and 1633 (C=O).

Monomer 2. A solution of 4-vinylbenzoic acid (1.13 g, 7.60 mmol), *N*-2-hydroxyethylcarbazole^{16b} (1.61 g, 7.60 mmol), DCC (2.35 g, 11.4 mmol), and DPTS (1.11 g, 3.80 mmol) in CH₂Cl₂ (15 mL) was stirred at room temperature overnight. The precipitate was filtered off, and the solvent was evaporated under reduced pressure to afford the product which was further purified by column chromatography (dichloromethane): 2.0 g (77% yield). ¹H NMR (400 MHz, CDCl₃) δ (ppm): 8.12 (d, 2H, ph-H), 7.78 (d, 2H, ph-H), 7.48–7.22 (m, 8H, ph-H), 6.73 (q, 1H, ph-CH=), 5.85 (d, 1H, =CH), 5.38 (d, 1H, =CH), 4.68 (s, 4H, -CH₂-). MS (EI, *m/z*): 341. Anal. Calcd: C 80.92%, H 5.61%, N 4.10%. Found: C 80.65%, H 4.95%, N 3.72%. IR (KBr, cm⁻¹): 1715 (C=O, ester), 1628 (C=C).

General Procedure for Polymerization. Monomers and AIBN in a ratio of 100:1 in DMF (20 wt %) were placed in a sealed tube and heated at 70 °C for 24 h. The product from the opened reaction tube was poured into methanol (e.g., 100 mL), and the ligand polymer was filtered off, washed with methanol, and dried in oven at 50–80 °C overnight.

Polymer 3a. The mole feed ratio of ligand monomer to comonomer is 1:6.5. Anal. Found: N 4.44%, C 79.49%, H 5.60%. ¹H NMR (400 MHz, DMSO-*d*₆) δ (ppm): 10.5 (s, 1H, -NH), 7–8 (m, 11H, ph-H), 6.4 (s, 3H, ph-H), 4.5 (s, 4H, -CH₂), 1–2 (s, 3H, -CHCH₂).

Polymer 3b. The mole feed ratio of ligand monomer to comonomer is 1:4. Anal. Found: N 5.08%, C 79.41%, H 5.46%. ¹H NMR (400 MHz, DMSO-*d*₆) δ (ppm): 10.5 (s, 1H, -NH), 6–8 (m, 14H, ph-H), 4.5 (s, 5H, -CH₂), 1–2 (s, 4H, -CHCH₂).

Polymer 3c. The mole feed ratio of ligand monomer to comonomer is 1:3. Anal. Found: N 5.28%, C 78.80%, H 5.44%. ¹H NMR (400 MHz, DMSO-*d*₆) δ (ppm): 10.5 (s, 1H, -NH), 6–8 (m, 13H, ph-H), 4.6 (s, 4H, -CH₂), 1–2 (s, 4H, -CHCH₂).

Polymer 3d. The mole feed ratio of ligand monomer to comonomer is 1:2. Anal. Found: N 5.63%, C 78.10%, H 5.61%. ¹H NMR (400 MHz, DMSO-*d*₆) δ (ppm): 10.5 (s, 2H, -NH), 7–8 (m, 6H, ph-H), 6.7 (s, 2H, ph-H), 1–2 (s, 3H, -CHCH₂).

General Procedure for Complexation of Ligand Polymers.^{3c} A solution of *cis*-Ru(bpy)₂Cl₂·2H₂O (0.23 g, 0.43 mmol), ligand polymer (0.21 mmol per the DCH group, according to elemental analysis), and sodium carbonate (0.06 g, 0.59 mmol) in a 30 mL of DMF were heated to reflux for 48 h under argon. After cooling to room temperature, a solution of ammonium hexafluorophosphate (1.5 g in 55 mL of water) was added. The red dark precipitate was filtered off and redissolved in acetone (20 mL). The ruthenium complex was then precipitated out with ether and dried under vacuum at room temperature (50% yield). The ruthenium content in complex polymers **4a–d** is listed in Table 1.

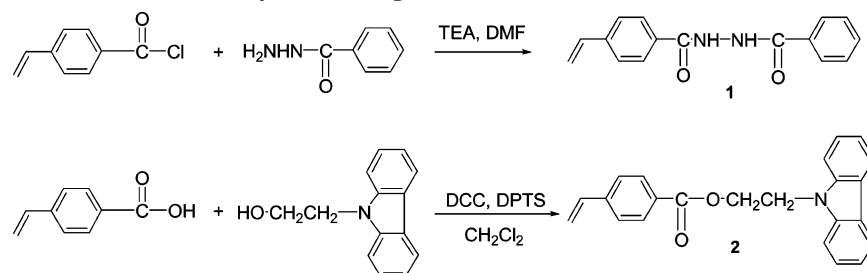
Complex **5** used in this study as a standard for CV characterization was synthesized according to the procedure described in our previous work.^{3a,b}

Results and Discussion

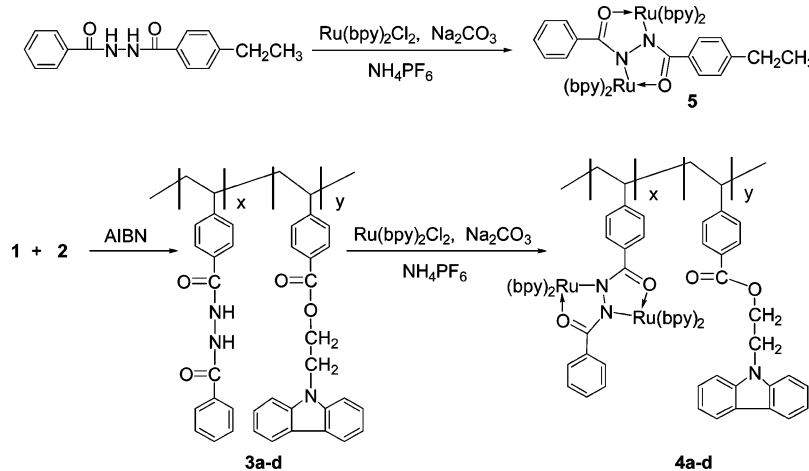
Synthesis and Characterization. There are generally two routes to the ruthenium complex polymers.^{3c,14} One is to directly polymerize a ruthenium complex monomer with or without a comonomer (**2**). Another route is based on postpolymerization or polymer transformation and involves the synthesis of the ligand polymer and subsequent complexation with Ru(bpy)₂Cl₂. In this study, we chose the postpolymerization route simply because of availability of desired monomers (Schemes 1 and 2). The choice of using a comonomer (**2**), 2-(9*H*-carbazol-9-yl)ethyl 4-vinylbenzoate, was made mainly by considering the fact that poly(vinylcarbazole) is a common and better matrix polymer for light-emitting small molecules and has been reported to be able to improve the performance (e.g., fast charging time) of a light-emitting electrochemical cell consisting of a ruthenium complex.¹⁵

The DCH ligand monomers **1** and **2** were prepared according to general procedures¹⁶ and polymerized using AIBN as initiator to produce ligand polymers **3a–d**. The feed ratios of monomer **1** to monomer **2** are 1:6.5, 1:4, 1:3, and 1:2 in polymerization. The corresponding ligand polymers **3a**, **3b**, **3c**, and **3d** were

Scheme 1. Synthesis of Ligand Monomer 1 and Comonomer 2



Scheme 2. Synthesis of Ligand Polymers and Complex Polymers and Structure of the Model Complex



obtained in good yields and found to have a relatively lower content of DCH moiety with the ratios of 1:19, 1:5.2, 1:4.3, and 1:3.2, respectively, as calculated from elemental analysis (Table 1). This indicates that monomer 2 is more reactive than monomer 1 under the given polymerization conditions. From GPC analysis, the number-average molecular weights of these ligand polymers are in a range of 24 000–42 000 with a polydispersity index (PDI) from 2.2 to 2.4 (Table 1). The structures of all the ligand polymers were consistent with the spectroscopic data (NMR and IR). DSC and TG analyses indicate the T_g of the ligand polymers about 150 °C and the onset temperature for 5% weight loss in air above 380 °C.

The complex polymers 4a–d were synthesized according to the procedure described in our previous work.^{3d} Since the ligand polymers are stable toward degradation under the same complexation conditions, the number-average molecular weights of these complex polymers are considered to be equal to those of the ligand polymers. The ruthenium content in the complex polymers was determined by ICP analysis (Table 1) and did not reach the theoretical values for complete complexation due to steric hindrance of the polymer backbone. All the complex polymers showed no clear glass transition and were stable to 350 °C in air.

Absorption, Electrochemical, and Spectroelectrochemical Studies. The UV–vis–NIR absorption spectra for the complex polymers in acetonitrile (1.2×10^{-4} mg/L) show two intense absorptions at 350 and 520 nm, attributed to the MLCT transition (Figure 1). Cyclic voltammograms (CV) were done using platinum electrodes against silver pseudoreference electrode in nitrogen-purged solution of 0.1 M Bu_4NPF_6 in acetonitrile. Complex 5 (Scheme 2) was used as the model complex and showed two quasi-reversible, one-electron oxidation processes in the positive potential region (Figure 2). The first oxidation ($^1E_{1/2}$) wave corresponds to the oxidation of the $\text{Ru}^{\text{II}}/\text{Ru}^{\text{III}}$ state to the $\text{Ru}^{\text{II}}/\text{Ru}^{\text{III}}$ state, while the second ($^2E_{1/2}$) is due to the further oxidation to the $\text{Ru}^{\text{III}}/\text{Ru}^{\text{IV}}$ state. The gap between the two oxidation potentials (ΔE) is about 0.60 V, which is close to those of other dinuclear DCH–Ru complexes.³ However, only broad CV of complex polymers could be obtained. In reference to the redox potentials ($^1E_{1/2}$ and $^2E_{1/2}$) of the model complex 5, the spectroelectrochemical measurements of the complex polymers were performed using an OTTE cell by applying different potentials. Since the spectroelectrochemical properties of all the complex polymers are quite similar, the absorption spectra of just one complex polymer (4d) in three oxidation states are presented in Figure 3. Two intense absorptions at 350 and 520 nm are assigned to the $\text{Ru}^{\text{II}}/$

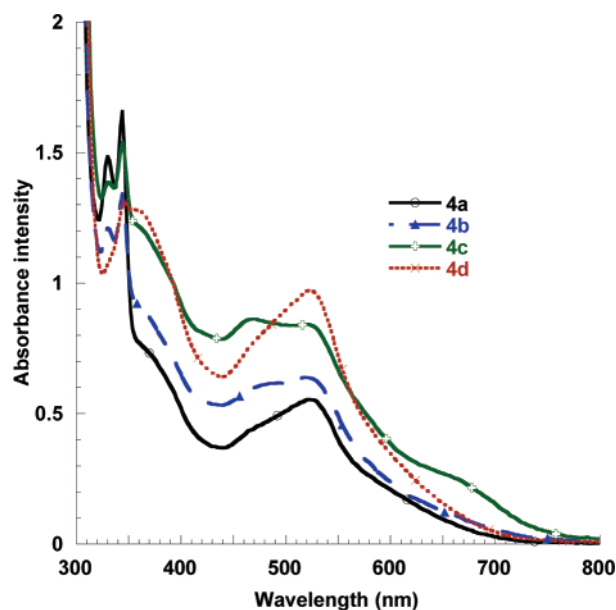


Figure 1. Absorbance spectra of complex polymers 4a–d in acetonitrile (1.2×10^{-4} mg/L).

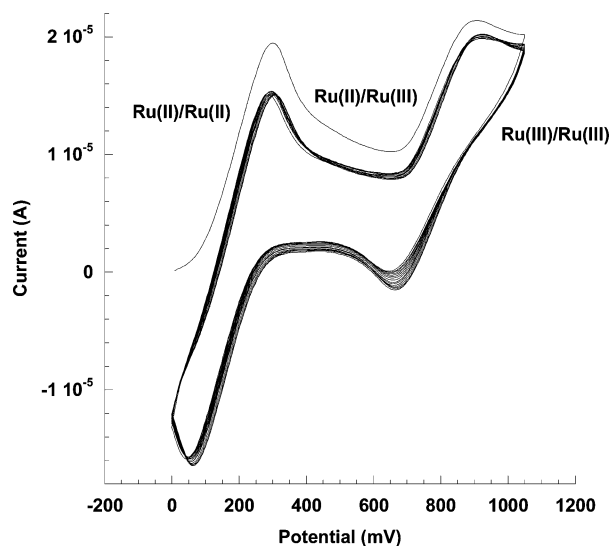


Figure 2. Cyclic voltammogram (30 cycles with a scan rate of 50 mV/s) of model complex **5** in acetonitrile containing 0.1 M Bu₄NPF₆.

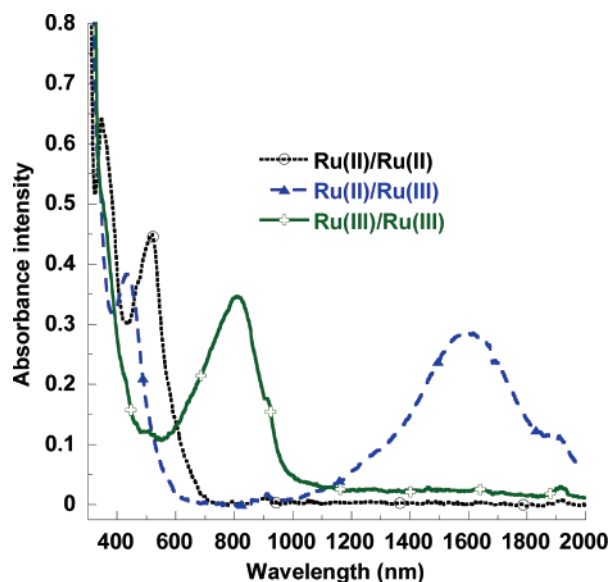


Figure 3. Absorption spectra of complex polymer **4d** in three oxidation states obtained in acetonitrile/0.1 M Bu₄NPF₆ using the OTTE cell.

Ru^{II} state of the complex polymers, while a broad NIR absorption from 1000 to 2000 nm with a maximal peak at 1600 nm is attributed to the MMCT band of the Ru^{II}/Ru^{III} mixed-valence state. Upon further oxidation to the Ru^{III}/Ru^{III} state, a new band at 800 nm appears due to a ligand-to-metal charge-transfer (LMCT) transition. These results indicate the complex polymers **4a–d** are NIR electrochromic at the telecommunication wavelength of 1550 nm, but the switching speed of the polymer films on the electrodes might be slow, given the observed broad CV traces, in comparison with other DCH–Ru complex polymer films reported before.^{3d}

Photoluminescent and Electroluminescent Properties. The PL of the complex polymers in acetonitrile (4.8×10^{-4} mg/L) was investigated under excitation of 520 nm light at room temperature. The PL spectra for all the complex polymers **4a–d** are virtually identical with a maximal peak at about 790 nm (Figure 4). On the basis of the previous study on the fluorescent ruthenium complexes,^{10–13} the excited-state metal-to-ligand (³-MLCT) of ruthenium-containing polymers **4a–d** should be responsible for the observed NIR PL. To demonstrate EL of complex polymers **4a–d**, a typical single-layer diode device

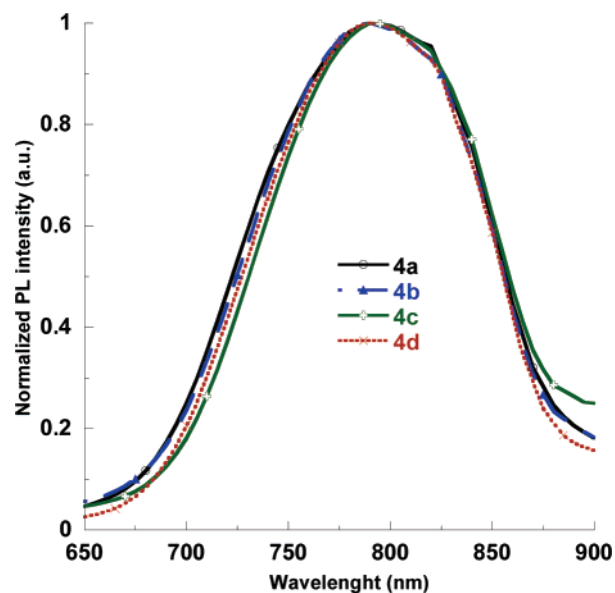


Figure 4. PL spectra of complex polymers **4a–d** in acetonitrile excited at 520 nm.

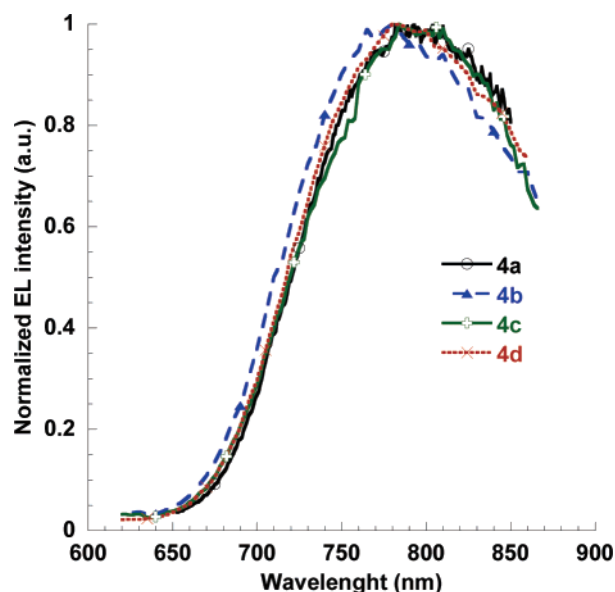


Figure 5. EL spectra of complex polymers (device structure: ITO/complex polymer/Au).

was fabricated with the structure of ITO/complex polymer/Au. All the complex polymers can be cast into a good film with a thickness of about 80 nm on ITO anode. A layer of gold (130 nm) as a cathode is deposited onto the polymer layer under a pressure of 3×10^{-7} Torr. The EL spectra (Figure 5) for all the complex polymers are similar to their PL spectra. The EL emission due to $\pi^* \rightarrow t_{2g}$ transition with a maximal peak at about 790 nm is among the longest EL emissions ever reported to date for the ruthenium complexes.

The temporal evolution of the current and radiance of the LED device based on polymer **4d** is shown in Figure 6 under different forward bias voltages. Upon application of a voltage, the current rapidly increases to a steady-state value, while the radiance initially follows the current but then decays exponentially with time, which is similar to other ruthenium complex-based devices reported in the literature.^{7a,12c,16} The solid-state LED devices operate in a mechanism similar to that for electrochemical cells. Unlike organic LED requiring low work-function cathodes (e.g., Ca), the devices containing redox

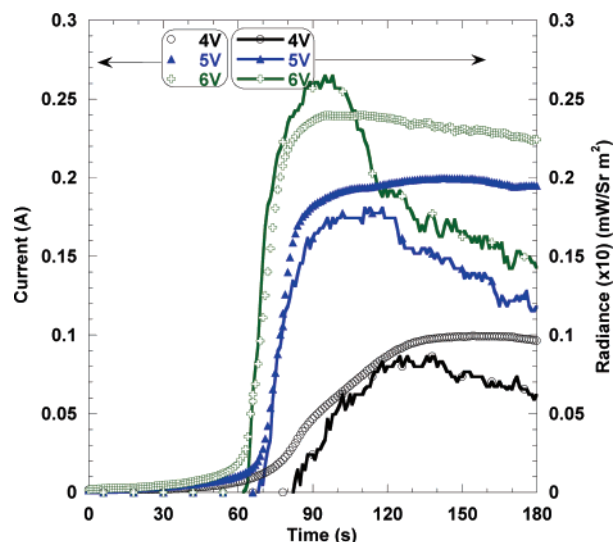


Figure 6. Temporal evolution of the current and radiance of the devices for complex polymer **4d** under different forward bias voltages.

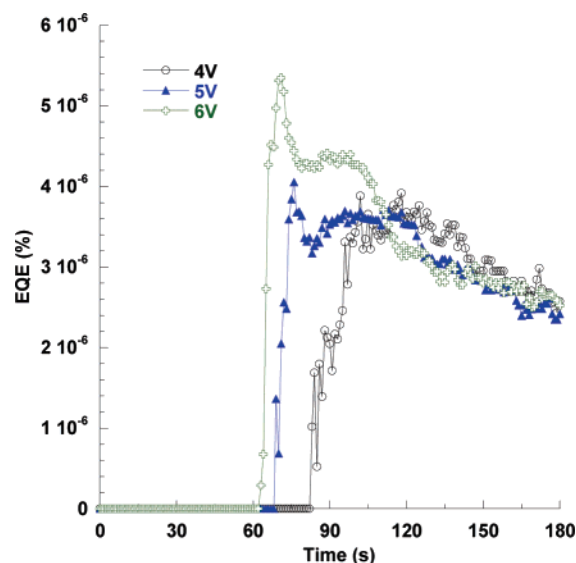


Figure 7. Temporal evolution of device EQE for complex polymer **4d** under different forward bias voltages.

ruthenium complex polymers can be made with an air-stable Au cathode. Upon applying a voltage, the counterions (PF_6^-) accumulate near the anode and deplete near the cathode, causing a lowering of the barriers for hole and electron injection and thus an increase in the current. When the anion distribution is in equilibrium at the electrodes, as dictated by the applied bias and the Coulombic interactions with the ionic and electronic charge in the device, a steady state is reached. It is believed that in the steady state the applied voltage drops at the contacts, and the holes and electrons move within the device by diffusion only.¹⁶ A higher applied voltage facilitates the accumulation of the PF_6^- ions at the anode, resulting in a faster device turn-on (Figure 6). The external quantum efficiency (EQE) of the devices for complex polymer **4d** was found to correlate with the applied voltages (Figure 7). Both the EL radiance and EQE begin to decay after the current is up to the steady state and decay faster under higher voltages. Using the other three complex polymers **4a–c** having less ruthenium content, much weaker EL and lower EQE were obtained for **4b** and **4c** at 6.5 V, and no EL emission was observed for **4a**.

Conclusions

Novel dinuclear ruthenium complex polymers with good thermal stability and film-forming ability were prepared and characterized. All the complex polymers **4a–d** are NIR electrochromic at 1600 nm and show photoluminescence (PL) and electroluminescence at the wavelengths around 790 nm, which may be potentially useful for NIR optical sensor, biomedical imaging, and telecommunication applications.

Acknowledgment. This work was supported by the National Natural Science Foundation of China (Project Nos. 20325415, 20228407) and the Natural Sciences and Engineering Research Council of Canada.

References and Notes

- (1) (a) Lim, Y. T.; Kim, S.; Nakayama, A.; Stott, N. E.; Bawendi, M. G.; Frangioni, J. V. *Mol. Imaging* **2003**, *2*, 50–64. (b) Kim, S.; Lim, Y. T.; Soltesz, E. G.; De Grand, A. M.; Nakayama, A.; Parker, J. A.; Mihaljevic, T.; Laurence, R. G.; Dor, D. M.; Cohn, L. H.; Bawendi, M. G.; Frangioni, J. V. *Nat. Biotechnol.* **2004**, *22*, 93–97.
- (2) (a) Kasack, V.; Kaim, W.; Binder, H.; Jordanov, J.; Roth, E. *Inorg. Chem.* **1995**, *34*, 1924–1933. (b) Kaim, W.; Kasack, V.; Binder, H.; Roth, E.; Jordanov, J. *Angew. Chem., Int. Ed. Engl.* **1988**, *27*, 1174–1176.
- (3) (a) Qi, Y.; Desjardins, P.; Meng, X. S.; Wang, Z. Y. *Opt. Mater.* **2002**, *21*, 255–263. (b) Qi, Y.; Desjardins, P.; Wang, Z. Y. *J. Opt. A: Pure Appl. Opt.* **2002**, *4*, S273–S277. (c) Qi, Y.; Desjardins, P.; Birau, M.; Wu, X.; Wang, Z. Y. *Chin. J. Polym. Sci.* **2003**, *21*, 147–152. (d) Qi, Y.; Wang, Z. Y. *Macromolecules* **2003**, *36*, 3146–3151. (e) Wang, Z. Y.; Zhang, J.; Wu, X.; Birau, M.; Yu, G.; Yu, H.; Qi, Y.; Desjardins, P.; Meng, X.; Gao, J. P.; Todd, E.; Song, N.; Bai, Y.; Beaudin, A. M. R.; LeClair, G. *Pure Appl. Chem.* **2004**, *76*, 1435–1443.
- (4) Rastegar, M. F.; Todd, E.; Tang, H.; Wang, Z. Y. *Org. Lett.* **2004**, *6*, 4519–4522.
- (5) Li, X.; Zeng, W.; Zhang, Y.; Hou, Q.; Yang, W.; Cao, Y. *Eur. Polym. J.* **2005**, *41*, 2923–2933. (b) Yang, R.; Tian, R.; Yan, J.; Zhang, Y.; Yang, J.; Hou, Q.; Yang, W.; Zhang, C.; Cao, Y. *Macromolecules* **2005**, *38*, 244–253. (c) Caño, T. D.; Hashimoto, K.; Kageyama, H.; Saja, J. A. D.; Aroca, R.; Ohmori, Y.; Shirota, Y. *Appl. Phys. Lett.* **2006**, *88*, 071117.
- (6) Curry, R. J.; Gillin, W. P. *Appl. Phys. Lett.* **1999**, *75*, 1380–1382. (b) Suzuki, H. *Appl. Phys. Lett.* **2000**, *76*, 1543–1545. (c) Slooff, L. H.; Polman, A.; Cacialli, F.; Friend, R. H.; Hebbink, G. A.; van Veggel, F. C. J. M.; Reinhoudt, D. N. *Appl. Phys. Lett.* **2001**, *78*, 2122–2124. (d) Ostrowski, J. C.; Susumu, K.; Robinson, M. R.; Therien, M. J.; Bazan, G. C. *Adv. Mater.* **2003**, *15*, 1296–1300. (e) Kang, T.-K.; Harrison, B. S.; Foley, T. J.; Kniefely, A. S.; Boncella, J. M.; Reynolds, J. R.; Schanze, K. S. *Adv. Mater.* **2003**, *15*, 1093–1097.
- (7) Elliott, C. M.; Pichot, F.; Bloom, C. J.; Rider, L. S. *J. Am. Chem. Soc.* **1998**, *120*, 6781–6784. (b) Rudmann, H.; Shimada, S.; Rubner, M. F. *J. Am. Chem. Soc.* **2002**, *124*, 4918–4921. (c) Xia, H.; Zhang, C.; Qiu, S.; Lu, P.; Zhang, J.; Ma, Y. *Appl. Phys. Lett.* **2004**, *84*, 290–292. (d) Gong, X.; Ng, P. K.; Chan, W. K. *Adv. Mater.* **1998**, *10*, 1337–1340. (e) Tung, Y.-L.; Lee, S.-W.; Chi, Y.; Chen, L.-S.; Shu, C.-F.; Wu, F.-I.; Carty, A. J.; Chou, P.-T.; Peng, S.-M.; Lee, G.-H. *Adv. Mater.* **2005**, *17*, 1059–1064.
- (8) Handy, E. S.; Pal, A. J.; Rubner, M. F. *J. Am. Chem. Soc.* **1999**, *121*, 3525–3528. (b) Gao, F. G.; Bard, A. J. *J. Am. Chem. Soc.* **2000**, *122*, 7426–7427. (c) Chan, W. K.; Ng, P. K.; Gong, X.; Hou, S. *Appl. Phys. Lett.* **1999**, *75*, 3920–3922.
- (9) Slinker, J.; Bernards, D.; Houston, P. L.; Abruña, H. D.; Bernhardt, S.; Malliaras, G. G. *Chem. Commun.* **2003**, 2392–2399.
- (10) Bergman, S. D.; Goldberg, I.; Barbieri, A.; Barigelletti, F.; Kol, M. *Inorg. Chem.* **2004**, *43*, 2355–2367. (b) Bergman, S. D.; Goldberg, I.; Barbieri, A.; Kol, M. *Inorg. Chem.* **2005**, *44*, 2513–2523.
- (11) Stadler, A.-M.; Puntoriero, F.; Campagna, S.; Kyritsakas, N.; Welter, R.; Lehn, J.-M. *Chem.—Eur. J.* **2005**, *11*, 3997–4009. (b) Ceroni, P.; Credi, A.; Balzani, V.; Campagna, S.; Hanan, G. S.; Arana, C. R.; Lehn, J.-M. *Eur. J. Inorg. Chem.* **1999**, 1409–1414.
- (12) Encinas, S.; Flamingni, L.; Barigelletti, F.; Constable, E. C.; Housecroft, C. E.; Schofield, E. R.; Figgemeier, E.; Fenske, D.; Neuburger, M.; Vos, J. G.; Zehnder, M. *Chem.—Eur. J.* **2002**, *1*, 137–150. (b) Beley, M.; Chodorowski, S.; Collin, J.-P.; Sauvage, J.-P.; Flamingni, L.; Barigelletti, F. *Inorg. Chem.* **1994**, *33*, 2543–2547. (c) Barbieri, A.; Ventura, B.; Barigelletti, F.; Nicola, A.; Quesada, M.; Ziessel, R. *Inorg. Chem.* **2004**, *43*, 7359–7368.

- (13) Welter, S.; Brunner, K.; Cola, L. *Nature (London)* **2003**, *421*, 54–57. (b) Bolink, H. J.; Cappelli, L.; Coronado, E.; Grt  zel, M.; Nazeeruddin, Md. K. *J. Am. Chem. Soc.* **2006**, *128*, 46–47. (c) Bernhard, S.; Barron, J. A.; Houston, P. L.; Abr  da, H. D.; Ruglovksy, J. L.; Gao, X.; Malliaras, G. G. *J. Am. Chem. Soc.* **2002**, *124*, 13624–13628. (d) Rudmann, H.; Shimada, S.; Rubner, M. F. *J. Am. Chem. Soc.* **2002**, *124*, 4918–4921.
- (14) Lee, J.-K.; Yoo, D.; Rubner, M. F. *Chem. Mater.* **1997**, *9*, 1710–1712. (b) Ng, W. Y.; Gong, X.; Chan, W. K. *Chem. Mater.* **1999**, *11*, 1165–1170. (c) Cho, Y.-S.; Ihn, C.-S.; Lee, H.-K.; Lee, J.-S. *Macromol. Rapid Commun.* **2001**, *22*, 1249–1253. (d) Cho, Y.-S.; Lee, H.-K.; Lee, J.-S. *Macromol. Chem. Phys.* **2002**, *203*, 2495–2500. (e) Yu, S. C.; Hou, S.; Chan, W. K. *Macromolecules* **1999**, *32*, 5251–5256.
- (15) Takane, N.; Gaynor, W.; Rubner, M. F. *Polym. Prepr. (Am. Chem. Soc. Polym. Div.)*, **2004**, *45*, 349.
- (16) Kikuchi, D.; Sakaguchi, S.; Ishii, Y. *J. Org. Chem.* **1998**, *63*, 6023–6026. (b) Bloxham, J.; Moody, C. J.; Slawin, A. M. Z. *Tetrahedron* **2002**, *58*, 3709–3720.

MA061751+